

## Noninnocent Behavior of Ancillary Ligands: Apparent Trans Coupling of a Saturated N-Heterocyclic Carbene Unit with an Ethyl Ligand Mediated by Nickel

Tobias Steinke,<sup>†</sup> Bryan K. Shaw,<sup>†</sup> Howard Jong,<sup>†</sup> Brian O. Patrick,<sup>†</sup>  
Michael D. Fryzuk,<sup>\*,†</sup> and Jennifer C. Green<sup>\*,‡</sup>

*Department of Chemistry, The University of British Columbia, 2036 Main Mall, Vancouver, BC V6T 1Z4,  
and Inorganic Chemistry Laboratory, University of Oxford, South Park Road, Oxford OX1 3QR, U.K.*

Received February 20, 2009; E-mail: fryzuk@chem.ubc.ca; Jennifer.Green@chem.ox.ac.uk

**Abstract:** Oxidative addition of the tridentate N-heterocyclic carbene (NHC) diphosphine ligand precursor ([PCP]H)PF<sub>6</sub> (**1**) ([PCP] = *o*-Pr<sub>2</sub>PC<sub>6</sub>H<sub>4</sub>(NC<sub>3</sub>H<sub>4</sub>N)*o*-C<sub>6</sub>H<sub>4</sub>P'Pr<sub>2</sub>) to Ni(COD)<sub>2</sub> results in the formation of the nickel(II) hydride complex ([PCP]NiH)PF<sub>6</sub> (**2**). This hydride undergoes a rapid reaction with ethylene to generate a nickel(0) complex in which an ethyl group has been transferred to the carbene carbon of the original NHC–diphosphine ligand. If the first intermediate is the anticipated square-planar nickel(II) ethyl species, then the formation of the product would require a process that involves a trans C–C coupling of the NHC carbon and a presumed Ni–ethyl intermediate. Deuterium-labeling studies provide evidence for migratory insertion of the added ethylene into the Ni–H bond rather than into the Ni–carbene linkage; this is based on the observed deuterium scrambling, which requires reversible β-elimination, alkene rotation, and hydride readdition. However, density functional theory studies suggest that a key intermediate is an agostic ethyl species that has the Ni–C bond cis to the NHC unit. A possible transition state containing two cis-disposed carbon moieties was also identified. Such a process represents a new pathway for catalyst deactivation involving NHC-based metal complexes.

### Introduction

One of the most exciting advances in transition-metal-catalyzed processes has been the move toward use of N-heterocyclic carbenes (NHCs) as ancillary ligands.<sup>1–7</sup> This has been driven by a number of factors, including the enhanced stability of NHC-containing complexes (particularly vs similar phosphine-based systems) and the enhanced reactivity of NHC-derived catalysts.<sup>8–10</sup> However, as spectator ligands, NHCs have shown some potential drawbacks, as the carbene moiety can participate in migratory insertion,<sup>11–13</sup>

reductive elimination,<sup>14</sup> and “wrong-way” binding via C–H bond activation.<sup>15</sup> Such noninnocent reactivities are likely sources of NHC-based catalyst deactivation.<sup>16</sup>

Incorporation of NHCs into chelating arrays has been shown to generate particularly robust catalyst systems.<sup>4</sup> For example, a palladium complex of a tridentate [CNC] system consisting of a pyridine flanked by two sterically unencumbered NHCs, has been reported to be stable to 180 °C in air and active for Heck catalysis.<sup>17</sup> Interestingly, stoichiometric reactions done independently have shown that this type of tridentate NHC system can behave noninnocently by migratory insertion or reductive elimination behavior. In both cases (Figure 1),<sup>11,14</sup> the NHC is positioned cis to the Pd–methyl unit, which is optimal for both of these processes.

Other tridentate ligand systems that incorporate NHCs are known,<sup>18</sup> and those with the NHC positioned as the central donor should be less susceptible to these kinds of deleterious processes.<sup>19,20</sup> In this paper, we document a C–C bond-forming process to generate a nickel(0) derivative that apparently involves the NHC moiety and the trans-disposed hydride ligand.

<sup>†</sup> The University of British Columbia.

<sup>‡</sup> University of Oxford.

- Herrmann, W. A. *Angew. Chem., Int. Ed.* **2002**, *41*, 1290–1309.
- Lappert, M. F. *J. Organomet. Chem.* **2005**, *690*, 5467–5473.
- Hu, X.; Meyer, K. *J. Organomet. Chem.* **2005**, *690*, 5474–5484.
- Pugh, D.; Danopoulos, A. A. *Coord. Chem. Rev.* **2007**, *251*, 610–641.
- Peris, E.; Crabtree, R. H. *Coord. Chem. Rev.* **2004**, *248*, 2239–2246.
- N-Heterocyclic Carbenes in Transition Metal Catalysis*; Glorius, F., Ed.; Springer: Berlin, 2007; Vol. 21.
- N-Heterocyclic Carbenes in Synthesis*; Nolan, S. P., Ed.; Wiley-VCH: Weinheim, Germany, 2006.
- Scholl, M.; Ding, S.; Lee, C. W.; Grubbs, R. H. *Org. Lett.* **1999**, *1*, 953–956.
- Chiu, P. L.; Lai, C.-L.; Chang, C.-F.; Hu, C.-H.; Lee, H. M. *Organometallics* **2005**, *24*, 6169–6178.
- Lee, M.-T.; Lee, H. M.; Hu, C.-H. *Organometallics* **2007**, *26*, 1317–1324.
- Danopoulos, A. A.; Tsoureas, N.; Green, J. C.; Hursthouse, M. B. *Chem. Commun.* **2003**, 756–757.
- Becker, E.; Stingl, V.; Dazinger, G.; Mereiter, K.; Kirchner, K. *Organometallics* **2007**, *26*, 1531–1535.
- Fantasia, S.; Jacobsen, H.; Cavallo, L.; Nolan, S. P. *Organometallics* **2007**, *26*, 3286–3288.

- Nielsen, D. J.; Magill, A. M.; Yates, B. F.; Cavell, K. J.; Skelton, B. W.; White, A. H. *Chem. Commun.* **2002**, 2500–2501.
- Crabtree, R. H. *J. Organomet. Chem.* **2005**, *690*, 5451–5457.
- Yang, X.; Hall, M. B. *J. Am. Chem. Soc.* **2008**, *130*, 1798–1799.
- Peris, E.; Loch, J. A.; Mata, J.; Crabtree, R. H. *Chem. Commun.* **2001**, 201–202.
- Mata, J. A.; Poyatos, M.; Peris, E. *Coord. Chem. Rev.* **2007**, *251*, 841–859.
- Zhou, Y.; Xi, Z.; Chen, W.; Wang, D. *Organometallics* **2008**, *27*, 5911–5920.
- Lee, H. M.; Zeng, J. Y.; Hu, C.-H.; Lee, M.-T. *Inorg. Chem.* **2004**, *43*, 6822–6829.

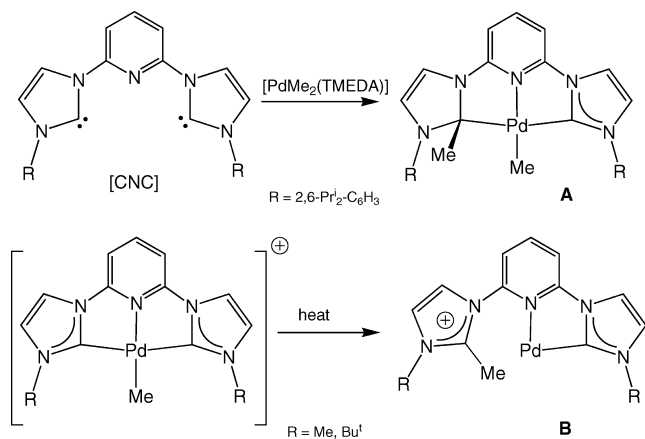
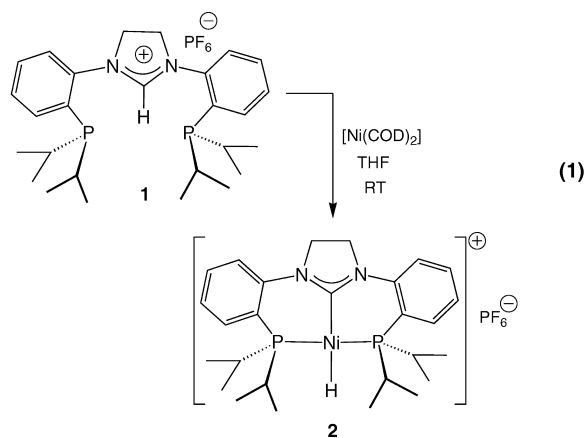


**Figure 1.** Noninnocent behavior of tridentate bis(NHC)pyridine ligands. The formation of **A** can be considered as a migratory insertion, whereas production of **B** formally corresponds to a reductive elimination.

Mechanistic and computational studies show that this process is unlikely to involve square-planar nickel(II) intermediates.<sup>21</sup>

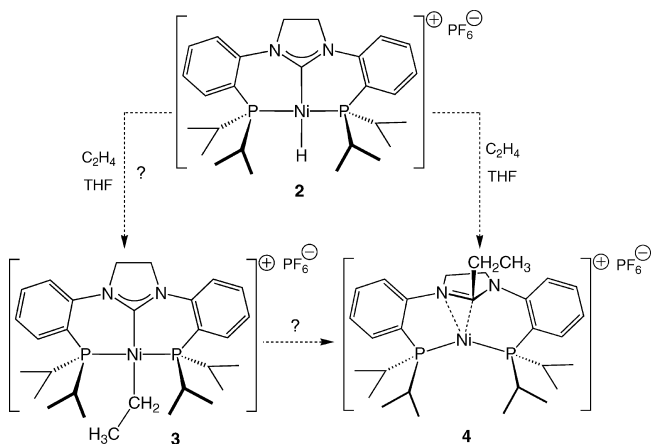
## Results and Discussion

**Experimental Studies.** We recently reported<sup>22</sup> on the preparation of the rigid tridentate ligand [PCP], which consists of a saturated NHC moiety flanked by two *o*-phosphinoaryl substituents, and its coordination chemistry with a variety of transition metals, including nickel. Reaction of the imidazolium salt ([PCP]H)PF<sub>6</sub> (**1**) {[PCP] = *o*-iPr<sub>2</sub>PC<sub>6</sub>H<sub>4</sub>(NC<sub>3</sub>H<sub>4</sub>N)-*o*-C<sub>6</sub>H<sub>4</sub>P<sup>i</sup>Pr<sub>2</sub>} with Ni(COD)<sub>2</sub> resulted in the formation of the nickel(II) hydride complex ([PCP]NiH)PF<sub>6</sub> (**2**) (eq 1), which was characterized by both NMR spectroscopy and X-ray crystallography.



In the process of examining the reactivity of the nickel hydride derivative, we added excess ethylene to a solution of **2** in tetrahydrofuran (THF) and observed a rapid color change from yellow to orange-red. Our expectation was the formation of a square-planar nickel(II) ethyl complex, ([PCP]NiEt)PF<sub>6</sub> (**3**), via migratory insertion of ethylene into the Ni–H bond.<sup>23</sup> Instead, the resultant product was the formally nickel(0) η<sup>2</sup>-iminium diphosphine complex shown as **4** in Scheme 1, which was formed in 70% isolated yield. That this was not the simple nickel(II) ethyl species **3** was evident from the <sup>1</sup>H NMR

**Scheme 1.** Reaction of Ethylene with Nickel Hydride Complex **2** to Produce **4** (The Role of Nickel Ethyl Complex **3** in this Transformation is Discussed in the Text)



spectrum, which showed rather broad signals, in particular, a set of two broad peaks due to the inequivalent methylene protons in the saturated carbene backbone, as well as resonances due to the inequivalent isopropyl substituents.

Single crystals obtained from THF were analyzed by X-ray diffraction; the solid-state molecular structure is shown in Figure 2 along with selected bond lengths and bond angles. What is immediately apparent is that C–C bond formation has occurred, resulting in attachment of the ethyl moiety to C1 (formerly the carbene carbon), and that this ethylimidazolium unit is now π-bound to the formally Ni(0) center. In the solid state, this η<sup>2</sup>-C=N interaction renders the two phosphine donors as well as the top and bottom of the π-bound heterocycle inequivalent. Interestingly, in solution, the <sup>31</sup>P{<sup>1</sup>H} NMR spectrum of **4** shows a singlet for the ligated phosphines even down to –80 °C, which suggests that fast exchange of the η<sup>2</sup>-C=N unit between N1 and N2 occurs on the NMR time scale. While this process equilibrates the two phosphine arms, it does not exchange the two isopropyl groups on each phosphorus, as they remain inequivalent even at higher temperatures because of the different faces of the coordinated heterocycle above and below the P1–Ni–P2 plane.

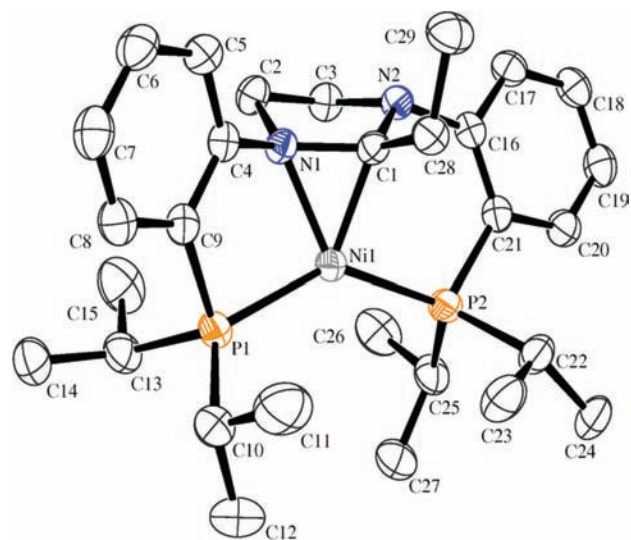


**Figure 2.** ORTEP diagram of the cation of **4**. Selected bond lengths (Å) and bond angles (deg): Ni1–P1, 2.2295(8); Ni1–P2, 2.1424(8); Ni1–N1, 1.967(2); Ni1–C1, 1.899(3); N1–C1, 1.436(3); P1–Ni1–P2, 137.33(3); N1–Ni1–C1, 43.54(10); N1–C1–N2, 107.3(2); P1–Ni1–N1, 89.68(7); C1–Ni1–P2, 92.35(8); C1–C28–C29, 115.3(2).

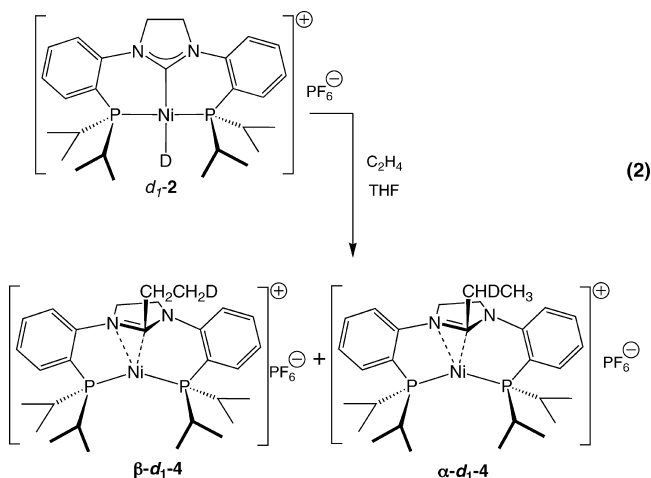
(21) Tatsumi, K.; Nakamura, A.; Komiya, S.; Yamamoto, A.; Yamamoto, T. *J. Am. Chem. Soc.* **1984**, *106*, 8181–8188.

(22) Steinke, T.; Shaw, B. K.; Jong, H.; Patrick, B. O.; Fryzuk, M. D. *Organometallics* **2009**, *28*, 2830–2836.

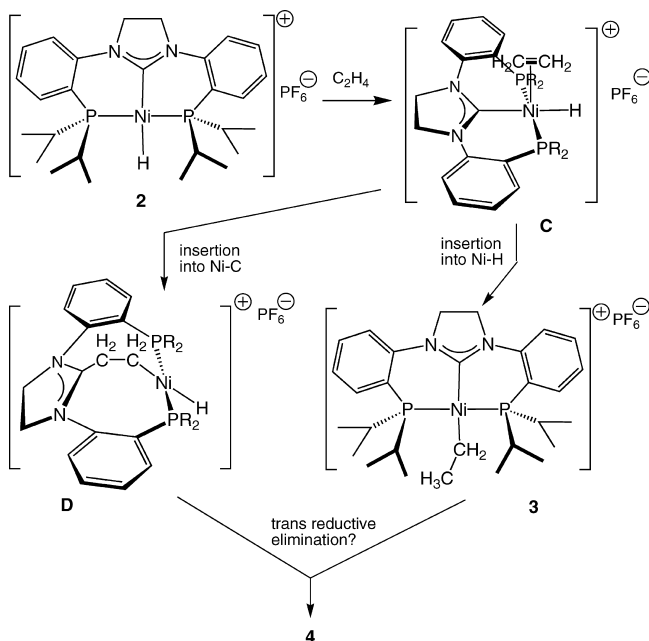
This product is somewhat reminiscent of the Pd(II)–[CNC] complex **A** described in Figure 1, for which migratory insertion of one of the flanking NHCs of the tridentate ligand into a Pd–Me bond has been documented.<sup>11</sup> However, what distinguishes the conversion of nickel(II) hydride **2** into the nickel(0) derivative **4** is that the central NHC donor was originally trans to the hydride and protected by the flanking *o*-phenyldiisopropylphosphine arms.

On the basis of a literature precedent,<sup>24</sup> we assumed that a likely intermediate would be the square-planar nickel ethyl complex **3**, which would be formed via migratory insertion of added ethylene into the Ni–H bond and could undergo a C–C coupling process to generate the observed nickel(0) product **4**. Another possible mechanism, but one with no precedent to our knowledge, would be direct insertion of ethylene into the Ni–carbene bond followed by C–H reductive elimination, which would also generate **4**. Both of these proposals are outlined in Scheme 2. The obvious problem with both proposed mechanisms is that reductive elimination processes normally require that the two ligands undergoing the rearrangement be cis-disposed, but in each process shown in Scheme 2, the square-planar nickel(II) center requires that the two ligands be trans-disposed. Even in the presence of excess ethylene, any putative five-coordinate intermediate could not rearrange to allow trans-to-cis isomerization of the migrating/eliminating ligands.<sup>21</sup> We carried out experiments to try to shed light on this process and perhaps distinguish the particular pathway (via **3** or **D** in Scheme 2) used in the process.

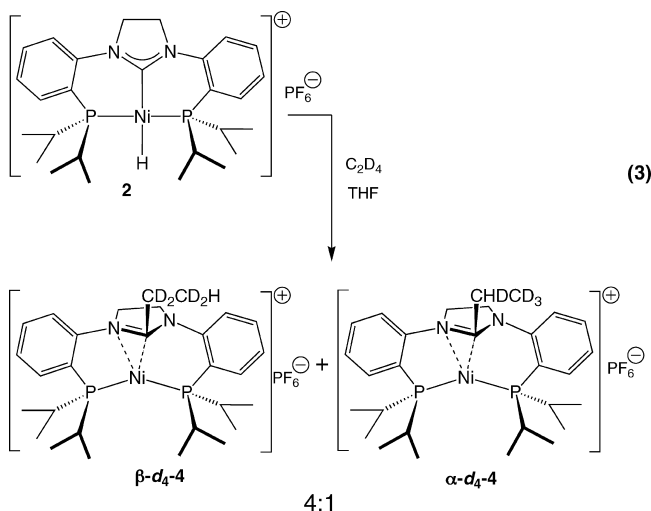
Labeling studies were performed in an effort to provide information on the mechanism and, in particular, to try to distinguish the site of insertion. The nickel deuteride *d*<sub>1</sub>-**2** was prepared simply by stirring the imidazolium salt in deuterated methanol (CD<sub>3</sub>OD) overnight. Addition of *d*<sub>1</sub>-**2** to Ni(COD)<sub>2</sub> resulted in the clean formation of *d*<sub>1</sub>-**2** with ~90% deuterium incorporation. Subsequent reaction of the deuteride with excess ethylene resulted in incorporation of deuterium mainly at the β position of the ethyl group in complex **4** (see eq 2), as indicated by decreases in the integrals of the <sup>1</sup>H NMR signals due to those hydrogens (~80% *d*<sub>1</sub> at this position); however, there was also evidence of deuterium incorporation in the methylene unit at the α position, as evidenced by a decrease in the integrals for these protons (between 15 and 25% *d*<sub>1</sub> at this position, depending on the experiment). However, we were unable to confidently confirm deuterium incorporation at the α position by either <sup>2</sup>H or <sup>13</sup>C NMR spectroscopy, even though the presence of deuterium at the expected β position was evident using both techniques. Selected <sup>2</sup>H and <sup>13</sup>C{<sup>1</sup>H} NMR spectra of a mixture of β-*d*<sub>1</sub>-**4** and α-*d*<sub>1</sub>-**4** are provided in the Supporting Information.



**Scheme 2.** Two Possible Mechanisms for Generating **4**: Associative Addition of Ethylene To Give the Five-Coordinate Species **C**, Which Can Insert into the Ni–H Bond To Form the Ni–Et Complex **3** or into the Ni–NHC Bond To Generate **D**



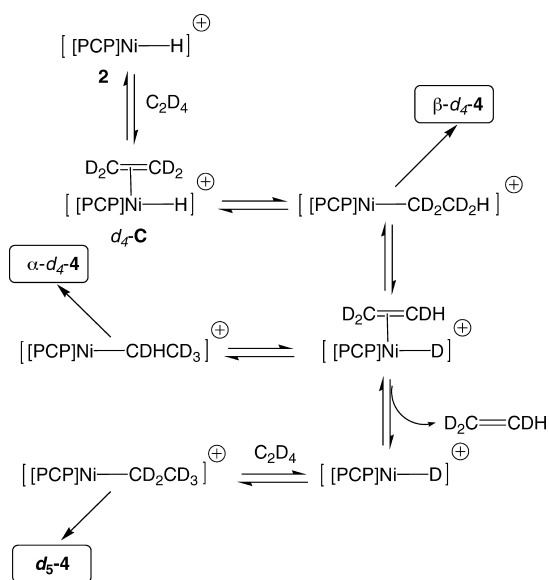
A complementary experiment was devised to confirm the presence of deuterium at the α-position. Addition of ethylene-*d*<sub>4</sub> to nickel hydride **2** resulted in the formation of β-*d*<sub>4</sub>-**4** and α-*d*<sub>4</sub>-**4**, as evidenced by <sup>1</sup>H NMR spectroscopy: clearly evident were a singlet at δ ~0.9 and a broad multiplet at δ ~1.5 for β-*d*<sub>4</sub>-**4** and α-*d*<sub>4</sub>-**4**, respectively, in a 4:1 ratio (see eq 3).



Interestingly, the amounts of α-*d*<sub>4</sub>-**4** and β-*d*<sub>4</sub>-**4** depended on the quantity of C<sub>2</sub>D<sub>4</sub> present; when slightly more than 1 equiv of C<sub>2</sub>D<sub>4</sub> was used, the quantities of these labeled materials matched that shown in eq 3, whereas when excess C<sub>2</sub>D<sub>4</sub> (>10 equiv) was used, considerably smaller proton integrals were observed; in particular, loss of the signal due to α-*d*<sub>4</sub>-**4** was readily apparent. We attribute this to the reversible β-elimination process with dissociation of ethylene-*d*<sub>3</sub> and incorporation of more deuterium via reaction with the excess C<sub>2</sub>D<sub>4</sub>. This process is described in Scheme 3.

Key to eliminating the possibility of direct insertion of ethylene into the Ni–carbene bond (see intermediate **D** in

**Scheme 3.** Reaction of  $C_2D_4$  with Nickel Hydride **2** To Generate Labeled Nickel(0) Derivatives: Loss of  $D_2C=CDH$  Occurs to a Small Extent and Results in the Formation of the Nickel Deuteride, Which Goes on To Generate  $d_5-4$



Scheme 2) are the production of  $\alpha-d_4-4$  and the observation of  $d_5-4$ , both of which can only occur via a series of reversible  $\beta$ -elimination and reinsertion steps into the Ni–H bond as shown in Scheme 3. There is no precedent for reversible deinsertion of a coordinated NHC with an alkene.

Attempts to extend this reaction to other simple alkenes have not been successful. There is no detectable reaction between nickel hydride **2** and propene under any conditions that we have employed to date.

**Computational Studies.** The deuterium-labeling studies provide strong evidence that migratory insertion occurs at the hydride site, but there is still the issue of the apparent trans coupling of the ethyl and NHC moieties at the nickel(II) center (Scheme 2). Monitoring the reaction mixture by NMR spectroscopy showed no evidence for the formation of nickel ethyl complex **3** (or any other intermediate), yet it seems to be implicated on the basis of the deuterium-scrambling studies discussed above. In order to provide some guidance concerning possible reaction pathways, density functional theory (DFT) calculations were performed on the starting hydride **2**, the observed ethylimidazolidinium complex **4**, and presumed intermediates using the ADF2007.01 program suite (BP86 functional, TZP basis set, frozen 1s cores on C and N, frozen 2p cores on P and Ni).<sup>25</sup> Shown in Figure 3 are the computed relative energies of the starting hydride **2**, the nickel ethyl complex **3**, and the nickel(0) product **4**.

The optimized structure  $2_C$  agrees quite well with the solid-state structure of this hydride;<sup>22</sup> the optimized structure of the final product has a slightly different conformation for the ethyl group as compared with the crystal structure of **4**, so it has been given the designation  $4'_C$ . The relative energies show that the

ethyl complex  $3_C$  is virtually isoenergetic with the starting hydride  $2_C$ . Most importantly, DFT correctly predicts that the nickel(0) product  $4'_C$  is energetically favorable relative to the starting hydride plus ethylene. Armed with these results, we examined possible intermediates between  $2_C$  and  $4'_C$ . The most relevant species that was uncovered is shown in Figure 4 as  $5_C$ , which is an agostic nickel ethyl complex different from the anticipated square-planar ethyl species **3**. In fact,  $5_C$  would result from the associative addition of ethylene to nickel hydride **2**, as the agostic H on the apical ethyl moiety of  $5_C$  is essentially trans to the NHC donor of [PCP], and  $5_C$  is very closely related to the putative intermediate **C** in Scheme 2.

To rationalize the observed deuterium scrambling, the agostic C–H interaction would have to dissociate and the methyl group rotate around the ethyl C–C bond to form the calculated apical ethyl transition state  $6_C$ , which could then revert to  $5_C$  with H and D exchanged. Also shown in Figure 4 is a possible transition state for migratory insertion of the ethyl group from the nickel to the NHC carbon atom; the calculated structure  $7_C$  is only 11.1 kcal/mol higher in energy than the starting hydride and is easily accessible given the parameters of the observed reaction.

Particularly gratifying is the fact that the originally anticipated but not observed nickel ethyl complex **3** (or  $3_C$ ), while accessible, is not required in order to generate the final nickel(0) ethylimidazolidinium complex **4**. This obviates the need to invoke a trans coupling of the ethyl group from the nickel to the NHC carbon. It is interesting to note that a space-filling model view of  $3_C$  shows considerable steric crowding of the ethyl group with the isopropyl groups on phosphorus (Figure 5).

The effect of steric interactions was examined computationally by recalculating the structures of the “isopropyl-free” complexes corresponding to those shown in Figure 3; in this case, the relative energies of the species in which the flanking phosphine units are  $PH_2$  instead of  $P^iPr_2$  are 0 kcal/mol for the hydride + ethene,  $-19.4$  kcal/mol for the nickel ethyl complex, and  $-17.8$  kcal/mol for the nickel(0) ethylimidazolidinium product. This shows that with no steric bulk, the square-planar nickel ethyl complex rather than the Ni(0) complex would be the thermodynamic product. Clearly, increasing the steric bulk at phosphorus has a profound effect on this process. This rationalizes why the reaction fails with slightly bulkier alkenes such as propene.

## Conclusions

The reaction of an alkene with a metal hydride to generate a metal alkyl derivative via migratory insertion is a fundamental process in organometallic chemistry<sup>24</sup> and a key step in numerous catalytic processes.<sup>26</sup> In the work reported here, the reaction of ethylene with a square-planar nickel(II) hydride complex involves a different process in which the trans-disposed NHC donor of the tridentate ligand is transformed via a C–C bond-forming process that generates an nickel(0) ethylimidazolidinium species. The results of deuterium-labeling studies are consistent with a process that involves a series of  $\beta$ -elimination, alkene rotation, and readdition steps that scrambles the labels. The actual C–C bond-forming step is best viewed as arising from an apical agostic ethyl complex that is positioned cis to the NHC carbon of the [PCP] ancillary ligand. This avoids invoking a trans coupling process,<sup>21</sup> which remains as an unreasonable

(23) Liang, L.-C.; Chien, P.-S.; Lee, P.-Y. *Organometallics* **2008**, *27*, 3082–3093.

(24) Collman, J. P.; Hegedus, L. S.; Norton, J. R.; Fincke, R. G. *Principles and Applications of Organotransition Metal Chemistry*; University Science Books: Mill Valley, CA, 1987.

(25) ADF, version 2007.01; Scientific Computing and Modelling NV: Amsterdam, 2007; <http://www.scm.com> and references therein. Full computational details are given in the Supporting Information.

(26) Parshall, G. W.; Ittel, S. D. *Homogeneous Catalysis*, 2nd ed.; Wiley Interscience: New York, 1992.

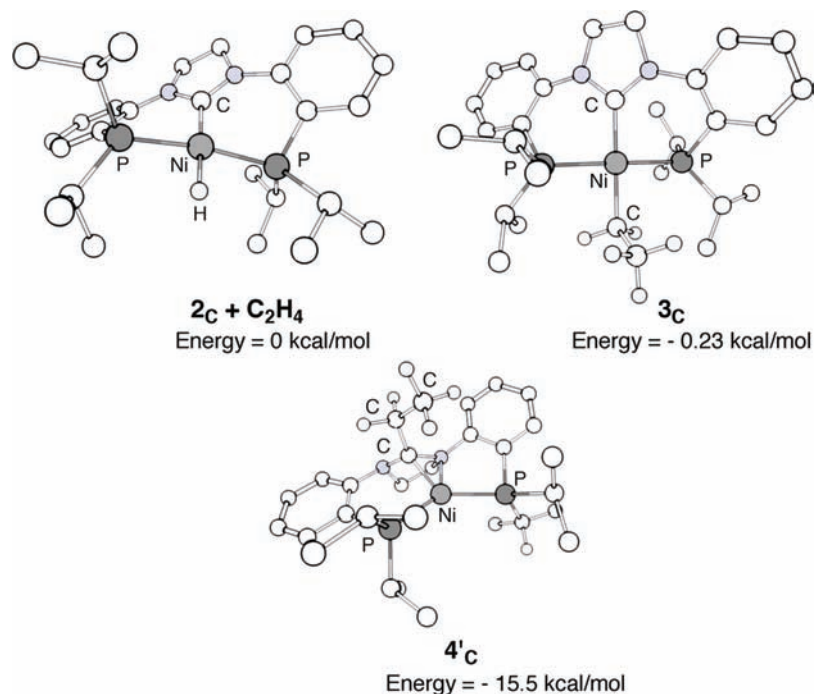


**Figure 3.** DFT-calculated structures and relative energies for hydride  $2_{\text{C}}$ , presumed intermediate ethyl  $3_{\text{C}}$ , and the final ethylimidazolidinium product  $4'_{\text{C}}$ ; the complexes are labeled with the subscript “C” to indicate that they are computed structures. Hydrogens other than those on Ni and the ethyl group have been omitted.

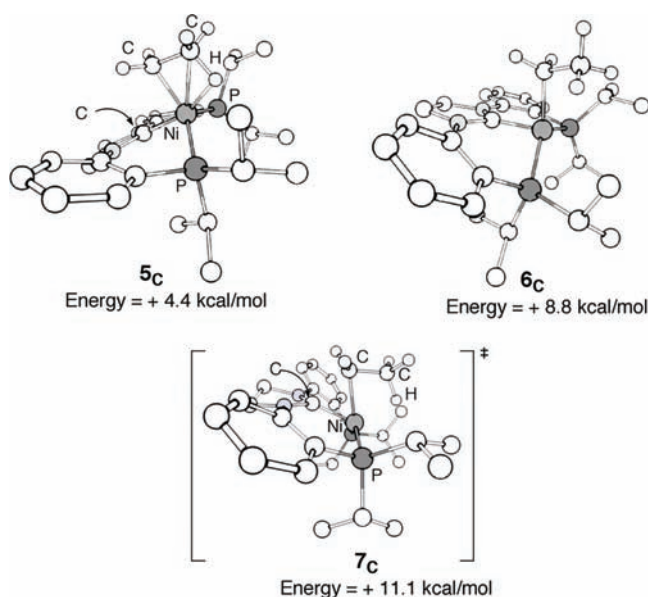


**Figure 4.** DFT-calculated structures and relative energies for the agostic ethyl complex  $5_{\text{C}}$ , the apical ethyl species  $6_{\text{C}}$ , and a potential transition-state structure  $7_{\text{C}}$ . The complexes are labeled with the subscript “C” to indicate that they are computed structures. All of the hydrogens except those on the ethyl group have been omitted.

assumption. DFT calculations show that the effect of steric interactions is the overriding feature of this process: the apical ethyl moiety is a result of the large isopropyl substituents on phosphorus,<sup>19</sup> which destabilize the formation of the square-planar nickel ethyl complex and cause the C–C bond-forming process to be the energetically favored pathway.

### Experimental Section

All of the reactions were performed using standard Schlenk techniques in an oxygen-free nitrogen atmosphere. NMR spectra

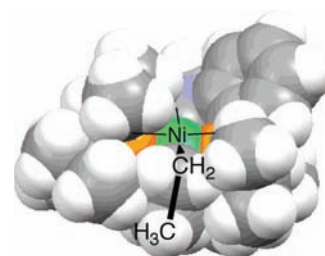


**Figure 5.** Space-filling model of the square-planar nickel(II) ethyl complex  $3_{\text{C}}$ , showing the severe steric crowding of the ethyl moiety lodged between the isopropyl groups on phosphorus.

were recorded on Bruker AV-400 instrument operating at 400.13 MHz ( $^1\text{H}$ ) and a Bruker AV-300 instrument operating at 300.13 MHz ( $^{13}\text{C}$  and  $^{31}\text{P}$ ). Chemical shifts are given relative to tetramethylsilane and were referenced to the residual proton solvent resonances as internal standards. THF was purchased anhydrous from Aldrich, sparged with nitrogen, and passed through columns containing activated alumina and molecular sieves. Deuterated solvents were dried by refluxing with  $\text{CaH}_2$ , then distilled trap-to-trap, and subjected to several freeze–pump–thaw cycles.  $([\text{PCP}]\text{NiH})\text{PF}_6$  (**2**) was synthesized according to a literature procedure.<sup>22</sup>  $\text{C}_2\text{D}_4$  (98%– $d_4$ ) was purchased from Cambridge Isotope Laboratories.

**Synthesis of  $([\text{PCP}]\text{NiD})\text{PF}_6$  ( $d_1$ -**2**).** The same procedure as described for **2** was used, except that **1** was replaced with the deuterated ligand  $([\text{PCP}]\text{D})\text{PF}_6$ .  $^2\text{H}$  NMR (THF, 61.43 MHz, 298 K):  $\delta$  –10.69 (t,  $^2J_{\text{PD}} = 8$  Hz, NiD).

**Synthesis of  $([\text{PCEtP}]\text{Ni})\text{PF}_6$  (**4**).** A yellow suspension of **2** (150 mg, 0.228 mmol) in THF (4 mL) was subjected to three freeze–pump–thaw cycles and then exposed to an atmosphere of ethylene. The color of the solution immediately changed to orange-red. The mixture was stirred for 30 min and then concentrated and slowly cooled to  $-30$  °C, giving orange-red crystals (109.5 mg, 70.0%).  $^1\text{H}$  NMR (THF- $d_8$ , 400.13 MHz, 298 K):  $\delta$  7.86 (br d, 2H, CH), 7.77 (br d, 2H, CH), 7.62 (t,  $J_{\text{HH}} = 7.4$  Hz, 2H, CH), 7.56 (t,  $J_{\text{HH}} = 7.3$  Hz, 2H, CH), 3.96 (br t, 2H,  $\text{CH}_2$ ), 3.75 (br t, 2H,  $\text{CH}_2$ ),

2.77 (br m, 2H, CH), 2.35 (br m, 2H, CH), 1.51 (q,  $J_{\text{HH}} = 7$  Hz, 2H, CH<sub>2</sub>), 1.36 (dd,  $J_{\text{HH}} = 6.4$  Hz,  $J_{\text{HP}} = 16.4$  Hz, 6H, CH<sub>3</sub>), 1.29 (dd,  $J_{\text{HH}} = 6.8$  Hz,  $J_{\text{HP}} = 17.3$  Hz, 6H, CH<sub>3</sub>), 1.18 (dd,  $J_{\text{HH}} = 7$  Hz,  $J_{\text{HP}} = 12.8$  Hz, 6H, CH<sub>3</sub>), 1.11 (dd,  $J_{\text{HH}} = 6.7$  Hz,  $J_{\text{HP}} = 15.7$  Hz, 6H, CH<sub>3</sub>), 0.96 (t,  $J_{\text{HH}} = 7.1$  Hz, 3H, CH<sub>3</sub>). <sup>13</sup>C{<sup>1</sup>H} NMR (THF-*d*<sub>8</sub>, 100.6 MHz, 298 K):  $\delta$  151.03 (t,  $J_{\text{CP}} = 9$  Hz), 134.68 (s), 133.36 (s), 129.80 (s), 129.37 (t,  $^2J_{\text{CP}} = 3$  Hz), 123.46 (s), 95.03 (s), 58.31 (s), 27.94 (t,  $J_{\text{CP}} = 9$  Hz), 24.58 (t,  $J_{\text{CP}} = 10.4$  Hz), 21.93 (t,  $^2J_{\text{CP}} = 4$  Hz), 20.64 (t,  $^2J_{\text{CP}} = 3$  Hz), 19.88 (t,  $^2J_{\text{CP}} = 4.7$  Hz), 19.77 (s), 10.60 (s). <sup>31</sup>P{<sup>1</sup>H} NMR (THF-*d*<sub>8</sub>, 161.9 MHz, 298 K):  $\delta$  36.8, -143.8 (sep). Anal. Calcd for C<sub>29</sub>H<sub>45</sub>N<sub>2</sub>F<sub>6</sub>P<sub>3</sub>Ni: C, 50.68; H, 6.60; N, 4.08. Found: C, 50.22; H, 6.38; N, 4.05.

**General Procedure for Ethylene Reactions.** A J. Young NMR tube with a total volume of 2.75 mL was charged with **2** or *d*<sub>1</sub>-**2** (30 mg, 0.05 mmol) and THF-*d*<sub>8</sub> (~1.25 mL). The suspension was then subjected to three freeze-pump-thaw cycles, and to the headspace was added a specified quantity of unlabeled or labeled ethylene gas, after which the tube was immediately sealed. The hydride dissolved upon shaking, and the mixture was monitored

by NMR spectroscopy. The diagnostic peaks of the ethyl unit at 1.51 (CH<sub>2</sub>) and 0.96 (CH<sub>3</sub>) in the <sup>1</sup>H NMR spectrum were used throughout to determine the amount of isotope incorporated. <sup>2</sup>H NMR (CH<sub>2</sub>Cl<sub>2</sub>, 61.43 MHz, 298 K):  $\delta$  1.53 (br s), 0.95 (br s).

**Acknowledgment.** We gratefully acknowledge funding from the NSERC of Canada and the Petroleum Research Fund, administered by the American Chemical Society. We also thank the Alexander von Humboldt Stiftung for a Feodor Lynen Fellowship for T.S.

**Supporting Information Available:** Crystallographic data for **4** (CIF); experimental details for the X-ray structure determination; details of the DFT results; and selected NMR spectra from the labeling experiments. This material is available free of charge via the Internet at <http://pubs.acs.org>.

JA901346G